Research Article

Molecular Pain
Volume 21: 1–15
© The Author(s) 2025
Article reuse guidelines:
sagepub.com/journals-permissions
DOI: 10.1177/17448069251321339
journals.sagepub.com/home/mpx
Sage

AMPK activation mitigates inflammatory pain by modulating STAT3 phosphorylation in inflamed tissue macrophages of adult male mice

Hongchun Xiang[1,2], Yuye Lan[2], Liang Hu[3], Renjie Qin[2], Hongping Li[4], Tao Weng[2], Yan Zou[2], Yongmin Liu[2], Xuefei Hu[2], Wenqiang Ge[2], Hong Zhang[2], Hui-Lin Pan[5], Na-na Yang[4], Wentao Liu[3], Guowei Cai[1], and Man Li[2]

Abstract

Inflammatory pain presents a significant clinical challenge. AMP-activated protein kinase (AMPK) is recognized for its capacity to alleviate inflammation by inhibiting transcription factors such as nuclear factor kappa B (NF-κB) and signal transducer and activator of transcription (STAT). Our prior research demonstrated that AMPK reduces inflammatory pain by inhibiting NF-κB activation and interleukin-1 beta (IL-1β) expression. However, the role of AMPK in regulating reactive oxygen species (ROS) and inducible nitric oxide synthase (iNOS) by modulating STAT3 phosphorylation in inflammatory pain remains inadequately understood. This study aims to investigate the role of AMPK in modulating STAT3 phosphorylation in the macrophages of inflamed tissues to mitigate inflammatory pain. A Complete Freund's Adjuvant (CFA)-induced inflammatory pain model was established by subcutaneous injection into the plantar surface of the left hindpaw of adult male mice. Behavioral tests of mechanical allodynia and thermal latency were used to determine nociceptive behavior. Immunoblotting quantified p-AMPK and iNOS expression levels. Nuclear translocation of p-STAT3(Ser727) and STAT3 in macrophages was assessed by western blot and immunofluorescence. ROS accumulation and mitochondrial damage in NR8383 macrophages were detected by flow cytometry. Lentivirus infection cells experiment was performed to transfect vectors encoding the STAT3 S727D mutants. Treatment with the AMPK activator AICAR alleviated CFA-induced inflammatory pain, enhanced AMPK phosphorylation, and reduced iNOS expression in inflamed skin tissues. AICAR effectively prevented STAT3 nuclear translocation while promoting the phosphorylation of STAT3 (Ser727) in the cytoplasm. In vitro studies with CFA-stimulated NR8383 macrophages revealed that AICAR increased STAT3(Ser727) phosphorylation, curtailed iNOS expression, and attenuated ROS accumulation and mitochondrial damage. Furthermore, the S727D mutation, which enhances STAT3 phosphorylation, replicated the protective effects of AICAR against CFA-induced oxidative stress and mitochondrial dysfunction. Our study shows that the AMPK acitvation downregulates iNOS expression by inhibiting the STAT3 nuclear translocation and promotes cytoplasmic STAT3(Ser727) phosphorylation, which reduces ROS expression and mitochondrial dysfunction, thereby alleviating inflammatory pain. These findings underscore the therapeutic potential of targeting AMPK and STAT3 pathways in inflammatory pain management.

Keywords

AMPK, STAT3, inflammatory pain, iNOS, ROS

Date Received: 21 November 2024; revised 8 January 2025; accepted: 27 January 2025

Creative Commons Non Commercial CC BY-NC: This article is distributed under the terms of the Creative Commons Attribution-NonCommercial 4.0 License (https://creativecommons.org/licenses/by-nc/4.0/) which permits non-commercial use, reproduction and distribution of the work without further permission provided the original work is attributed as specified on the SAGE and Open Access pages (https://us.sagepub.com/en-us/nam/open-access-at-sage).

Introduction

Inflammatory pain is a common form of chronic clinical pain.[1] It is caused by hypersensitivity of peripheral sensory nerve fibers stimulated by immune cells and inflammatory mediators.[2] Tissues damage lead to the release of various mediators from damaged cells and adjacent non-neural cells, such as astrocytes, microglia, platelets and immune cells. Inflammatory mediators in the extracellular environment increase the sensitivity of nociceptive neurons.[3] In formalin-induced inflammatory pain model, inhibition of interleukin-1 β (IL-1β), tumor necrosis factor-α (TNF-α), inducible nitric oxide synthetase (iNOS) and other inflammatory mediators significantly alleviate inflammatory pain.[4] Also, macrophages release inflammatory mediators and nitric oxide, which play an important role in inflammation and pain.[5,6]

AMP-activated protein kinase (AMPK) is a member of the family of metabolically sensitive protein kinases, which contains α -catalytic subunits and β-and γ-regulatory subunits.[7] AMPK activation can inhibit a variety of different pro-inflammatory signal cascades, including pro-inflammatory mechanistic target of rapamycin complex 1 (mTORC1), nuclear factor kappa B (NF-κB) and Janus kinase-signal transducer and activator of transcription (JAK-STAT) pathway.[8–11] Our previous study has shown that AMPK activation attenuates inflammatory pain through inhibiting NF-κB activation and IL-1β expression.[12] However, the AMPK-STAT pathway in inflammatory pain is unclear.

STAT3 is a member of the signal transducer and activator of transcription (STAT) family, and usually transmits signals from activated receptors or intracellular kinases to the nucleus, thus activating and regulating gene transcription.[13] Phosphorylation of STAT3 at Ser727 (p-STAT3) enhances transcription activity of STAT3.[14] In addition, $ZnCl_2$ promotes the phosphorylation of STAT3 in the cytoplasm, and reduces the mitochondrial damage and accumulation of reactive oxygen species (ROS) to alleviate the inflammatory injury.[15] Since both iNOS and ROS play an important role in inflammatory pain,[16–18] it is possible that AMPK activation alleviates inflammatory pain via inhibiting STAT3 nuclear translocation and enhancing STAT3 phosphorylation in the cytoplasm, thus inhibiting iNOS and ROS production.

Therefore, in the present study, we first determine whether AMPK activation alleviates pain hypersensitivity and inhibits the expression of iNOS in CFA-induced inflamed skin tissues. We then determine whether AICAR inhibits nuclear translocation of STAT3 and promotes the phosphorylation of STAT3 at Ser727 in the cytoplasm of macrophages, thus inhibiting the expression of iNOS and production of ROS and the subsequent mitochondrial damage of macrophages caused by CFA.

Materials and methods

Animal models

The experimental protocol was approved by the Animal Care and Use Committee at Huazhong University of Science and Technology (2022 Ethics No.3603) and conformed to the ethical guidelines of the International Association for the Study of Pain.[19] The experiments were carried out in strict accordance with the ethical guidelines of the International Association for the Study of Pain. Male C57BL / 6 mice (8–9 weeks old) were purchased from Beijing Vital River Laboratory Animal Technology Co., Ltd. Five mice were housed in each cage for 12 h light and 12 h dark(ambient temperature was 22–24℃), and had free access to water and food. Before final experiments, all mice were adapted to the environment first. As reported previously,[3] 25 μl CFA (Sigma, F5881-10 ml) was subcutaneously injected into the plantar of the left hindpaw to induce inflammatory pain, and 25 μl normal saline (N.S.) was

[1]Department of Acupuncture-Moxibustion, Union Hospital, Tongji Medical College, Huazhong University of Science and Technology, Wuhan, Hubei, P. R. China
[2]School of Basic Medicine, Tongji Medical College, Hubei key Laboratory of Drug Target Research and Pharmacodynamic Evaluation, Huazhong University of Science and Technology, Wuhan, China
[3]Department of Pharmacology, School of Basic Medicine, Nanjing Medical University, Nanjing, China
[4]International Acupuncture and Moxibustion Innovation Institute, School of Acupuncture- Moxibustion and Tuina, Beijing University of Chinese Medicine, Beijing, China
[5]Department of Anesthesiology and Perioperative Medicine, The University of Texas MD Anderson Cancer Center, Houston, TX, USA

Corresponding Authors:
Na-na Yang, International Acupuncture and Moxibustion Innovation Institute, School of Acupuncture- Moxibustion and Tuina, Beijing University of Chinese Medicine, No. 11 Bei San Huan Dong Lu, Beijing, 100029, China.
Email: 1254614551@qq.com

Wentao Liu, Department of Pharmacology, School of Basic Medicine, Nanjing Medical University, 101 Longmian Avenue, Nanjing, 211166, China.
Email: wtliu@njmu.edu.cn

Guowei Cai, Department of Acupuncture-moxibustion, Union Hospital, Tongji Medical College, Huazhong University of Science and Technology, No.1277 Jiefang Ave, Wuhan, 430022, China.
Email: cgw645@163.com

Man Li, School of Basic Medicine, Tongji Medical College, Hubei key Laboratory of Drug Target Research and Pharmacodynamic Evaluation, Huazhong University of Science and Technology, No.13 Hankong Road, Wuhan, 430030, China.
Email: liman73@mails.tjmu.edu.cn

injected in mice as the control group.AICAR (#9944) was obtained from Cell Signaling Technology, and AICAR (20 μg/20μl) was administrated 7 days after CFA injection.

Nociceptive behavior test

The baseline threshold of pain was measured 3 days before injection of CFA, and the threshold of the third day was taken as the baseline. Before testing the baseline values of mechanical allodynia and thermal hyperalgesia, all mice were adapted to the test environment for 30 min. The "up and down" method was used to determine the mechanical pain threshold of mice.[20] After 30 min of acclimation, we used von Frey (Stoelting, wood Dale, Italy) to stimulate vertically the plantar surface of the left hind paw for 5 s, and the rapid withdrawal or claw retraction of the hindpaw was considered a positive response. The von Frey test was repeated twice, and the average value was used as the mechanical threshold. Hotplate test was used to measure the thermal pain threshold, and the surface was maintained at 53°C. When the mice were placed on the hotplate, the latency of rapid paw withdrawal was considered the positive response. We set 20 s as the cutoff to prevent tissue damage.[21] The hotplate test was repeated every 5 min for three times and the average value was calculated.

Western blot

According to the experimental design, after the treatment in vivo, the mouse tissues were obtained for Western blot. Mice were anesthetized with excess sodium pentobarbital, and local inflammatory skin tissues were removed immediately and minced with scissors. After the treatment, the NR8383 cells were centrifuged at 1000 rpm for 5 min to collect the sediments. The tissues or NR8383 cells were then lysed by adding RIPA Lysis Buffer (10 μl/mg for tissues, 100 μl for cells in a well of six-well plates, #P0013B, Beyotime Biotechnology, China) with 1mM protease and phosphatase inhibitor cocktail (Guge Biotech, Wuhan, China). The lysate was centrifuged with 12,000 g (4℃, 15min) and the supernatant was collected. The protein contents of supernatant were detected by BCA kit(#P0012, Beyotime Biotechnology, China). Protein solution was boiled for 5 min at 95°C with 1/4 volume 5x loading buffer (Guge Biotech, Wuhan, China) and added to SDS-PAGE. Then, we transferred the proteins to the PVDF membrane(Millipore Corp.). The membranes were incubated with 5% skim milk or 5% BSA for 1 h at room temperature. The membrane was probed with the following primary antibodies: p-AMPK (Thr172) (Cell Signaling Technology, #2535, 1:1000); AMPK (Cell Signaling Technology, #2532, 1:1000); p-STAT3 (Ser727) (Abcam, #ab30647, 1:1000); STAT3 (Abcam, #68153, 1:1000); iNOS (Abcam, #178945, 1:1000); Histone-3 (Proteintech, #Cat. No.10265-1-AP, 1:10000); GAPDH (Proteintech, #Cat.No. 60004-1-Ig, 1:8000); β-actin (Santa Cruz Biotechnology, sc-47778, 1:10000). Secondary antibodies are anti-rabbit HRP and anti-mouse HRP (Beijing Kerui, 1:20000). Western blot analysis was used to assess the proteins of cytoplasm and nuclear extracts in local inflammatory tissues and NR8383 cells. We used Nucleoprotein and Cytoplasmic Protein Extraction Kit (#P0027, Beyotime Biotechnology, China) to extract nuclear and cytoplasmic proteins.

Quantitative polymerase chain reaction (qPCR)

Total RNA was isolated from local inflammatory skin tissues and NR8383 cells using Trizol Reagent (Invitrogen, TRIzol® Reagent, #15596-018). Spectrophotometer (Thermo Scientific, USA) was used to quantify the concentration of the total RNA. We used Hifair® II 1st Strand cDNA Synthesis SuperMix for qPCR (gDNA digester plus) for reverse transcription of total RNA to cDNA. We used Cham QTM Universal SYBR® qPCR Master Mix(Nanjing, China) on the Applied Biosystems QuantStudio 7 Flex (Thermo Fisher) for qPCR. Expression values of the iNOS mRNA were normalized to the corresponding mRNA levels of β-actin. We used $2^{-\Delta\Delta Ct}$ method to calculate relative expression levels of iNOS. The following are sequence-specific primers used: mouse iNOS FORWARD5'-3' CGGACGAGACGGATAGGCAG AG, iNOS REVERSE 5'-3' GGAAGGCAGCGGGCA CATG; mouse β-actin FORWARD 5'-3' GTGCTATGTT GCTCTAGACTTCG, β-actin REVERSE 5'-3' ATGCCAC AGGATTCCATACC.

Immunofluorescence labeling

After the drug treatment and behavioral tests, mice were anesthetized with excess sodium pentobarbital and were transcardially perfused with 37 °C saline followed by 4% paraformaldehyde in 0.1 M phosphate buffer (pH, 7.4; 4 °C). The local inflammatory skin tissues were quickly removed and post-fixed for 8h in the same fixative solution and cryoprotected in 20% and 30% sucrose in 0.1 M phosphate buffer for 24 h at 4 °C separately. The slices were cut to 15 μm using a cryostat (−20℃), and were mounted on a gelatin-coated slide and air dried for 6 h. For cell experiments, the cells were seeded into a 24 well plate with polylysine (0.01%)-coated slides, and then treated with drugs. At the end of the experiment, cells were fixed with 4% paraformaldehyde for 15 min, and washed with 0.01M PBS. The sections were washed in 0.1 M PBS and blocked for 1 h with 5% donkey serum (0.2% tween-20) in 0.01M PBS and then incubated with primary antibodies at 4°C overnight. The primary antibodies used included rabbit anti-p-AMPK (Abcam, #ab23875, 1:250), mouse anti-CD68 (Abcam, #ab955, 1:200), rabbit anti-p-STAT3 (Ser727) (Abcam, #ab30647, 1:300), rabbit anti-STAT3(Abcam, #68153, 1:300). The secondary antibodies used were donkey anti-rabbit IgG conjugated with Dylight 594 (Jackson Immuno Research, USA, 1:600) and donkey anti-mouse IgG conjugated with Dylight 488 (Jackson Immuno Research, USA, 1:600). Sections were incubated with DAPI for the nucleus staining for 5 min and then washed three times in 0.01M PBS for 5 min. Sections were cover-slipped with an anti-quenching mounting media. Images were acquired using a fluorescence microscope (BX51, Olympus, Japan) and were analyzed by using NIH ImageJ software (Bethesda, MD, USA).

Cell culture and treatment

A macrophage cell line (NR8383) was purchased from Procell (Procell, Wuhan, China) and cultured in HyClone™ DMEM high glucose medium (GE healthcare life sciences, HyClone Laboratories, USA) with penicillin/streptomycin (100 U/10 mg/mL, #C0222, Beyotime Biotechnology, China) and 20 % (v/v) fetal calf serum (Biological Industries, Kibbutz Beit, Israel). Cells were grown in 50 ml flasks under standard cell culture conditions (37 °C, 5%CO_2).

To determine whether AICAR induces activation of AMPK to decrease iNOS expression, NR8383 cells were treated with AICAR(0.5 mM) and Compound C (Abcam, #ab120843, 20 μM) before N.S.(Control) or CFA (100 μg/ml) treatment. NR8383 cells were exposed to CFA or vehicle for 24 h before being collected for western blot and flow cytometry.

Lentivirus transfection

The wild type (WT) control vector and vectors encoding the STAT3 Ser727 mutants were transfected into NR8383 cells according to the manufacturer's instruction. Briefly, cultured NR8383 cells were transfected for 48 h with the expression vectors for STAT3 S727D (Lentivirus vector encoding a m-Cherry–STAT3 fusion protein that carries a serine-to-aspartate substitution at codon 727-m-Cherry–STAT3 S727D) and WT STAT3 (Lentivirus vector encoding a m-Cherry–STAT3 fusion protein). The expression of m-Cherry-STAT3 and m-Cherry-STAT3 S727D was detected by fluorescence microscope. All vectors were constructed by Shanghai Genechem Technology Co., Ltd, China. The transfection efficiency (70%–80%) was evaluated by the percentage of cells with m-Cherry 48 h after transfection. The cells were collected for immunofluorescence and flow cytometry at the end of treatment.

Measurement of intracellular ROS

We used dye 2′,7′-dichlorofluorescein diacetate (DCFDA) (#S0033, Beyotime Biotechnology, China) to measure intracellular ROS. NR8383 cells were loaded with DCFH-DA (10 μM). DCFH-DA was diluted with serum-free medium and incubated for 30 minutes at 37℃. Then, cells were washed and resuspended with 0.01M PBS. Finally, we used BD LSRFortessa™, Special Order Research Product (FITC channel) to detect the fluorescence intensity of DCF (marking ROS). Flow Jo 7.6 was used to analyze data.

Measurement of mitochondrial dysfunction

Mito-Tracker Red CMXRos (#C1049, Beyotime Biotechnology, China) plays a role in labeling the mitochondria with biological activity and detecting the change of mitochondrial membrane potential. The normal cells show strong red fluorescence, and cells with mitochondrial membrane potential dysfunction show weaken red fluorescence. NR8383 cells were loaded with Mito-Tracker Red CMXRos (200 nM). Mito-Tracker Red CMXRos was diluted with complete medium and incubated for 30 minutes at 37℃. Then, cells were washed and resuspended with 0.01M PBS. Finally, we used BD LSRFortessa™, Special Order Research Product (PE-Texas Red-A channel) to detect the fluorescence intensity. Flow Jo 7.6 was used to analyze data.

Statistical analyses

All data were expressed in mean ± SEM and analyzed with SPSS, version 26.0. Two-way analysis of variance (ANOVA) followed by Bonferroni's post hoc test was used to determine statistical difference in the thermal latency and withdrawal thresholds between different groups. One-way ANOVA and Newman Keuls post hoc test were used to analyze the protein level and fluorescence intensity. The difference between two groups was analyzed using unpaired Student's t test. $P < 0.05$ was considered to be statistically significant.

Results

Subcutaneous injection of the AICAR alleviated CFA-induced pain hypersensitivity

Mice that received CFA injection exhibited mechanical allodynia and thermal hyperalgesia. A single subcutaneous administration of AICAR at day 7 after CFA injection significantly suppressed mechanical allodynia and thermal hyperalgesia (Figure 1(a) and (b)). AICAR treatment also markedly promoted the phosphorylation of AMPK (Figure 1(c)–(e)). Immunocytochemical labeling showed the co-labeling of macrophage and p-AMPK in local inflammatory skin tissue. Immunofluorescence analysis showed that AICAR can significantly promote the phosphorylation of AMPK in $CD68^+$ macrophages (Figure 1(f)). The results suggested that AICAR reduced inflammatory pain and induced activation of AMPK in local inflammatory skin tissues.

Activation of AMPK by AICAR significantly inhibited the expression of iNOS

Our experimental hypothesis is that activating AMPK in macrophages will reduce pain, as iNOS is a marker of pro-inflammatory macrophages. CFA injection significantly increased the protein and mRNA of iNOS. Treatment with AICAR by a single subcutaneous injection at day 7 after CFA injection significantly inhibited the expression levels of iNOS and mRNA of iNOS (Figure 1(g)–(i)).

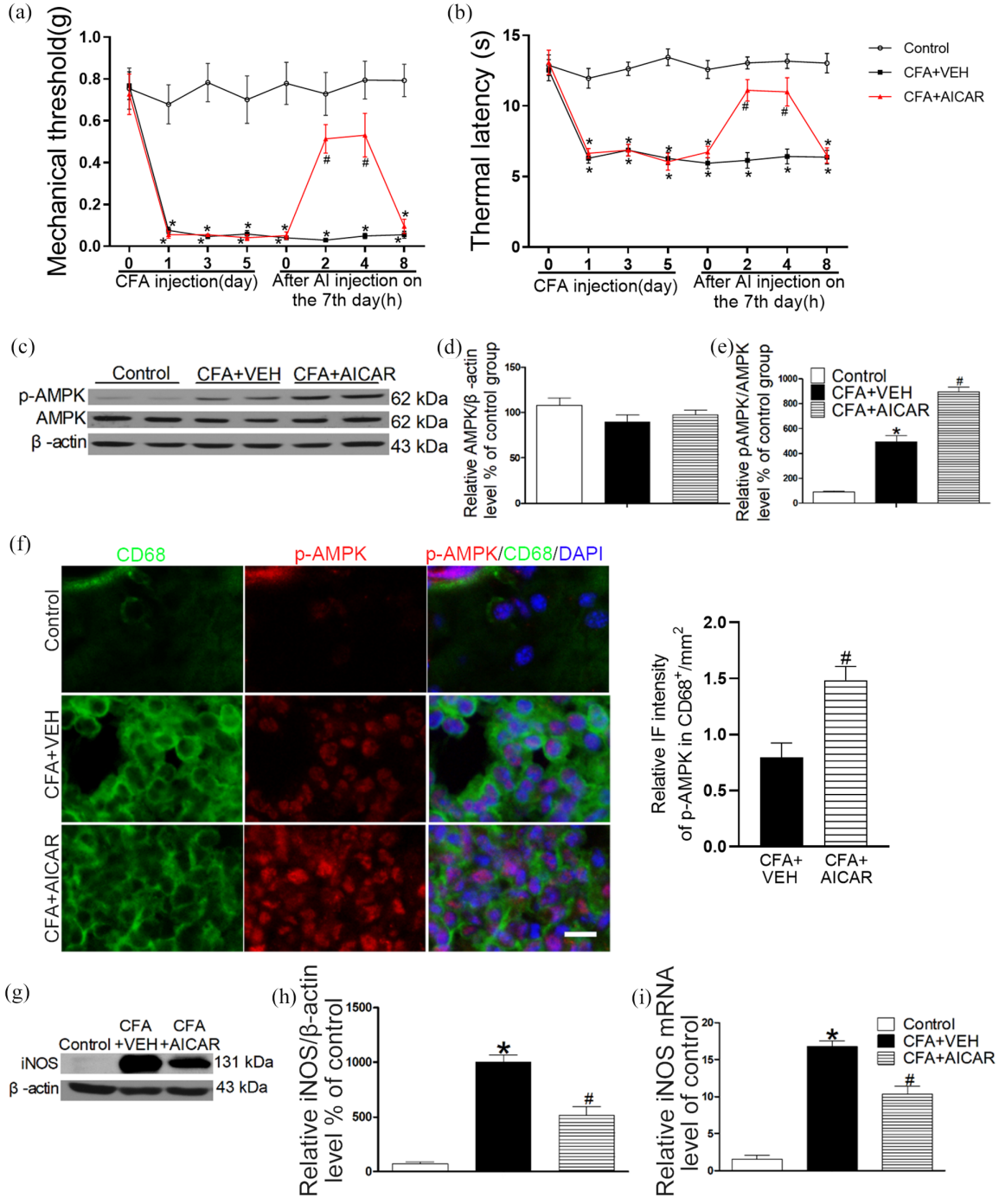

Figure 1. AICAR reduces inflammatory pain and increases AMPK phosphorylation, and inhibits protein and mRNA levels of iNOS in inflamed skin tissues. (a, b) Mechanical allodynia and thermal hyperalgesia were measured at 2, 4, and 8 h after treatment with AICAR or vehicle (N.S.) in the 7th day. AICAR (20 μg/20 μl) was injected locally into the inflammatory site at day 7 after CFA injection. *$P < 0.05$ versus Control group and #$P < 0.05$ vs. CFA+VEH group (n=8 per group, two-way ANOVA). (c–e) Gel images and group data showing changes in AMPK/p-AMPK in inflamed skin tissues ($n = 3$). Local inflammatory skin tissues were collected for Western blot 2 h after treatment with AICAR or vehicle. *$p < 0.05$ versus Control group and #$p < 0.05$ versus CFA+VEH group (one-way ANOVA). (f) Immunofluorescence images show co-localization of CD68 (green), p-AMPK (red) and DAPI in inflammatory skin tissues. Quantitative analysis shows the relative immunofluorescence (IF) intensity of p-AMPK in $CD68^+$ macrophages. Scale bar represents 50 μm. (g, h) Gel images and group data show iNOS proteins in inflamed skin tissues ($n = 3$). AICAR (20 μg/20 μl) was injected locally at day 7 after CFA-induced inflammation. Local inflammatory skin tissues were collected for Western blot and qPCR 2 h after treatment with AICAR or vehicle. (i) mRNA level of iNOS in inflamed skin tissues($n = 3$). *$p < 0.05$ versus Control group and #$p < 0.05$ versus CFA+VEH group (one-way ANOVA). VEH is the vehicle of AICAR (0.01 M PBS).

Activation of AMPK inhibited STAT3 nuclear translocation in macrophages and promoted STAT3 (Ser727) phosphorylation in macrophage cytoplasm

In CFA-induced inflammatory pain model, CFA significantly increased the level of p-STAT3 (Ser727), and AICAR further increased p-STAT3 (Ser727) in the total protein of inflammatory skin tissues (Figure 2(a) and (c)). There was no significant change in the total protein level of STAT3 in the control group, CFA and CFA plus AICAR group (Figure 2(a) and (b)).

We also detected STAT3 and p-STAT3 (Ser727) in cytoplasmic and nuclear. CFA significantly increased the level of p-STAT3 (Ser727) and STAT3 in nuclear of inflammatory skin tissues. AICAR reversed the effect of CFA (Figure 2(d)–(f)). Meanwhile, compared with the CFA model group, AICAR significantly increased the p-STAT3(Ser727) level in the cytoplasmic protein of inflammatory skin tissues CFA (Figure 2(g)—(i)). Immunofluorescence labeling showed the STAT3 and phosphorylation of STAT3 (Ser727) in $CD68^+$ macrophages. Immunofluorescence analysis showed that AICAR significantly inhibited the nuclear translocation of p-STAT3 and STAT3 in $CD68^+$ macrophages (Figure 2(j) and (k)). These results suggested that CFA induced the nuclear translocation of STAT3 in local inflammatory skin tissue, and increased level of p-STAT3 (ser727) in the nuclei. AMPK activation promoted the phosphorylation of STAT3 (Ser727), and increased the phosphorylation of p-STAT3 (Ser727) in the cytoplasm, and inhibited nuclear translocation of STAT3.

AMPK activation in NR8383 macrophages promoted the phosphorylation of STAT3 (Ser727) in cytoplasm and inhibited the nuclear translocation of STAT3 and the expression of Inos

Compared with the CFA model group, AICAR significantly inhibited the expression of iNOS and promote the phosphorylation of STAT3 (Ser727), and had no effect on STAT3. Compound C, an AMPK antagonist, reversed the action of AICAR (Figure 3(a)–(d)). It was confirmed that the activation of AMPK promoted the phosphorylation of STAT3 (Ser727) and inhibited the expression of iNOS in macrophages.

Compared with the control group, CFA significantly increased the levels of p-STAT (Ser727) and STAT3 in the nuclei, and decreased the levels of p-STAT3(Ser727) and STAT3 in the cytoplasm. Compared with CFA group, AICAR significantly decreased the levels of p-STAT3 (Ser727) and STAT3 in the nuclei, and increased the levels of p-STAT3 (Ser727) and STAT3 in the cytoplasm. AMPK antagonist, Compound C, reversed the effects of AICAR (Figure 4(a)–(e)). Immunofluorescence labeling showed the distribution of p-STAT3 (Ser727) and STAT3 in the cytoplasmic and nuclei of NR8383 macrophages (Figure 4(f)).

Specific activation of AMPK alleviated ROS accumulation and mitochondrial damage induced by CFA in NR8383 macrophages

It has been reported that $ZnCl_2$ treatment promotes the phosphorylation of STAT3 (Ser727) in the cytoplasm, and attenuates the mitochondrial damage and ROS accumulation to alleviate the inflammatory damage in the rat model of myocardial ischemia-reperfusion injury.[15] Compared with the control group, the fluorescence intensity of ROS in CFA group significantly increased, and the fluorescence intensity of Mito tracker red CMXRos in CFA group significantly decreased. Compared with CFA group, ROS fluorescence intensity of CFA plus AICAR group significantly decreased, and the fluorescence intensity of Mito tracker red CMXRos significantly increased. Compound C significantly reversed the effect of AICAR (Figure 5(A)–(d)). These results suggested that CFA induced ROS accumulation and mitochondrial damage in NR8383 macrophages. Activation of AMPK attenuated ROS accumulation and mitochondrial damage in NR8383 macrophages induced by CFA.

STAT3 phosphorylation mutation (S727D) reduced ROS accumulation and mitochondrial damage in NR8383 induced by CFA

The Ser727 site of STAT3 was mutated to aspartate to induce constitutive STAT3 phosphorylation. As reported previously,[15,22] the Ser727 site of STAT3 was mutated to aspartate as continuous phosphorylation of STAT3. We used m-Cherry-STAT3 S727D plasmid (m-Cherry STAT3 WT as negative control) for transfection with lentivirus in NR8383 macrophages. Compared with the control group, the ROS level in CFA plus WT group significantly increased. Compared with CFA plus WT group, the ROS level in CFA plus S727D group significantly decreased (Figure 6(a) and (b)). At the same time, we tested the effect of S727D on mitochondrial damage. Compared with CFA plus WT group, the fluorescence intensity of Mito tracker red CMXRos in CFA plus S727D group significantly increased (Figure 6(C)–(e)). These results indicated that AMPK activation promoted the phosphorylation of STAT3 (Ser727) to alleviate ROS accumulation and mitochondrial damage in macrophages caused by CFA (Figure 7).

Discussion

AMPK (adenosine monophosphate activated protein kinase) is a kinase that mainly regulates energy homeostasis. Phosphorylation of Thr172 site is a marker of AMPK activation.[23] In recent years, many studies have shown that AMPK

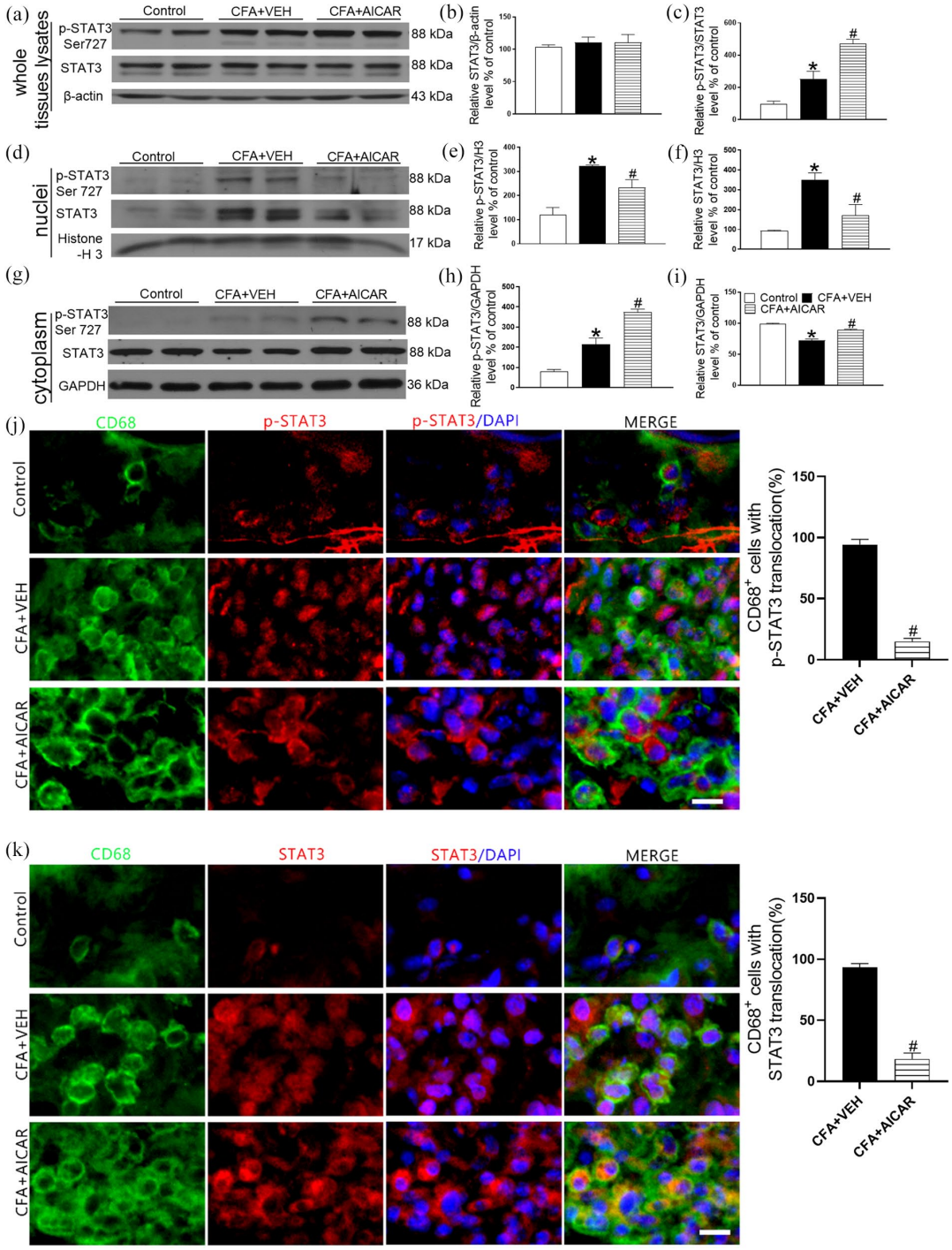

Figure 2. AICAR inhibits STAT3 nuclear translocation and promotes STAT3 (Ser727) phosphorylation in the cytoplasm of inflammatory skin tissues. (a–c) Gel images and group data of p-STAT3 (Ser727) and STAT3 in total protein of inflamed skin tissues ($n = 3$). (d–f) Gel images and group data of STAT3, p-STAT3 (Ser727) nuclear proteins and a nuclear reference protein Histone-3 (H3) in inflammatory skin tissues($n = 3$). (g–i) Gel images and group data of STAT3, p-STAT3 (Ser727) proteins and an internal reference GAPDH in cytoplasm skin tissues($n = 3$) respectively. AICAR (20 μg/20 μl) was injected locally at day 7 after CFA-induced inflammation. Local inflammatory skin tissues were collected to extract total protein, cytoplasmic and nuclear proteins for western blot 2 h after AICAR treatment. *$p < 0.05$ versus Control group and #$p < 0.05$ versus CFA+VEH group (one-way ANOVA). VEH is the vehicle of AICAR (0.01 M PBS). (j, k) Immunofluorescence images show subcellular distribution and co-localization of p-STAT3 (Ser727) (red), STAT3 (red), macrophage (CD68) (green) and DAPI(blue) in inflamed skin tissues($n = 3$ repeats). Immunofluorescence analysis shows that AICAR affects the nuclear translocation of p-STAT3 and STAT3 in CD68 cells. Scale bar, 50 μm. VEH is vehicle, which is the vehicle of AICAR, sterile 0.01M PBS.

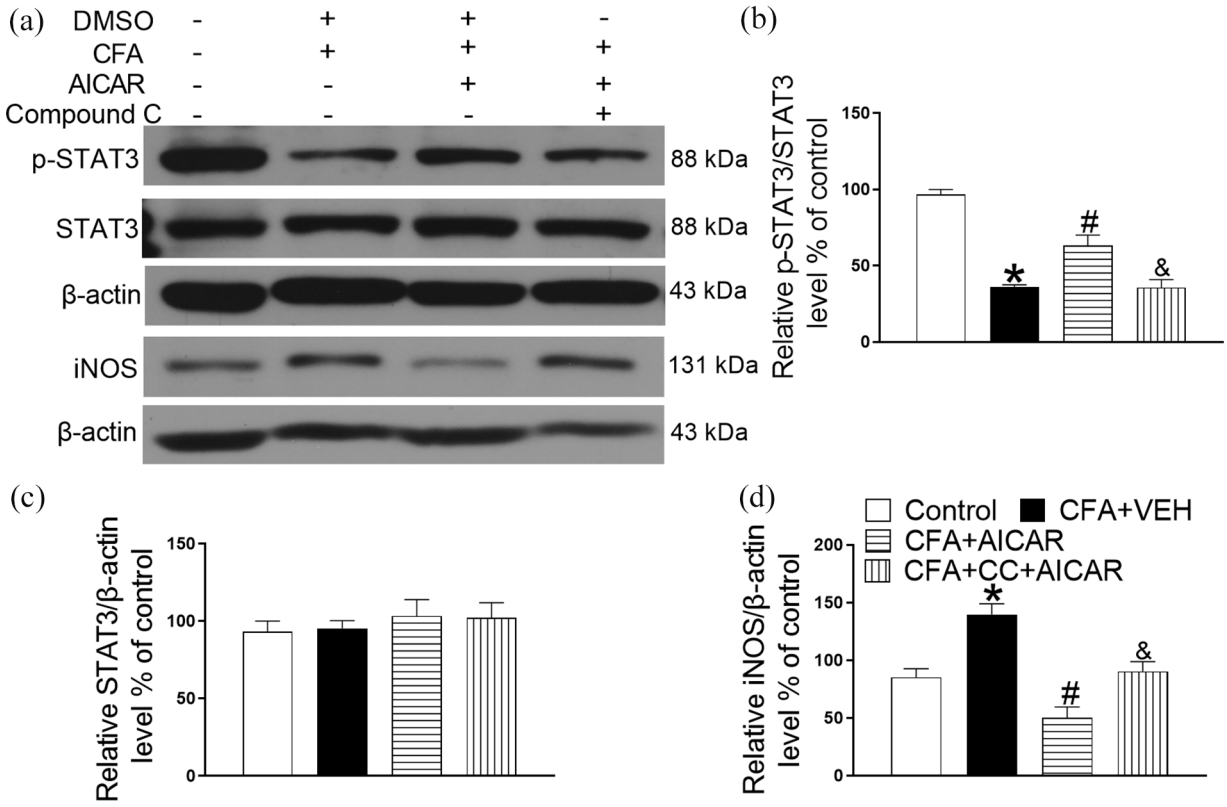

Figure 3. AICAR increases STAT3 (Ser727) phosphorylation and inhibits iNOS expression in NR8383 macrophages treated with CFA. Western blot was carried out 24 h after CFA induced inflammatory response. Representative gel images (a) and group data (b–d) show the expression of p-STAT3(Ser727), STAT3, iNOS and β-actin in NR8383 cells 24h after AICAR treatment ($n = 3$ per group). *$p < 0.05$ versus Control group, #$p < 0.05$ vs. CFA+VEH group and &$p < 0.05$ versus CFA+AICAR group (one-way ANOVA). VEH is the vehicle of AICAR (0.01 M PBS). CC, Compound C.

activation has anti-inflammatory and analgesic effects.[24,25] In this study, we investigated the novel mechanism by which AMP-activated protein kinase (AMPK) activation modulates the STAT3 to produce analgesic effects in CFA-induced inflammatory pain model. Our findings revealed that AMPK, activated by AICAR, inhibited STAT3's nuclear translocation and reduced the phosphorylation of p-STAT3 (Ser727) within the nuclei, consequently leading to the downregulation of inducible nitric oxide synthase (iNOS) overexpression. Additionally, AMPK activation facilitated cytoplasmic phosphorylation of STAT3 (Ser727), thereby mitigating ROS accumulation and alleviating mitochondrial dysfunction. This study unveils a new pathway through which AMPK exerts its anti-inflammatory and analgesic effects.

The phosphorylation of α-catalyzed threonine residues (Thr172) is a more effective regulator than allosteric activation, which can increase AMPK activity by nearly 100 times.[26] In pain model induced by spared nerve injury, activation of AMPK reduces the excitability of dorsal root ganglion neurons to relieve pain.[27] In the model of acute incision-induced pain in mice, local administration of resveratrol cream or systemic administration of metformin activates AMPK to alleviate pain.[28] When AMPKα is knocked out, the nociceptive response is enhanced in inflammatory pain model mice.[29] In the rat model of temporomandibular joint osteoarthritis, AMPK activation mediates the inhibition of IL-1β and nitric oxide to relieve the nociceptive pain.[30] In this study, subcutaneous injection of AICAR activated AMPK to alleviate CFA-induced pain hypersensitivity. It is in line with previous reports. AICAR activated AMPK in macrophage($CD68^+$), and inhibited iNOS expression of inflammation skin tissues of CFA-induced. We know that iNOS is marker of pro-inflammatory M1 macrophages and is involved in pain hypersensitivity.[5,31,32] Next, we investigated the mechanism of AMPK activation regulating iNOS expression.

There is a conserved SH2 (SRC homology 2) domain and a C-terminal tyrosine residue (Y705) in the primary amino acid sequence of STAT3. Phosphorylation of STAT3 (Y705) is the key factor to activate STAT3 transcription function.[33] STAT3 is a transcription factor that interacts with peptide receptors on the cell surface and mediates extracellular signals such as cytokines and growth factors. Specifically, under the stimulation of cytokines, STAT3 tyrosine phosphorylation has transcription activity, and nuclear translocation of STAT3 dimer achieves the transcription of target genes.[34,35] In addition, phosphorylation of STAT3 (Ser727) enhances transcription

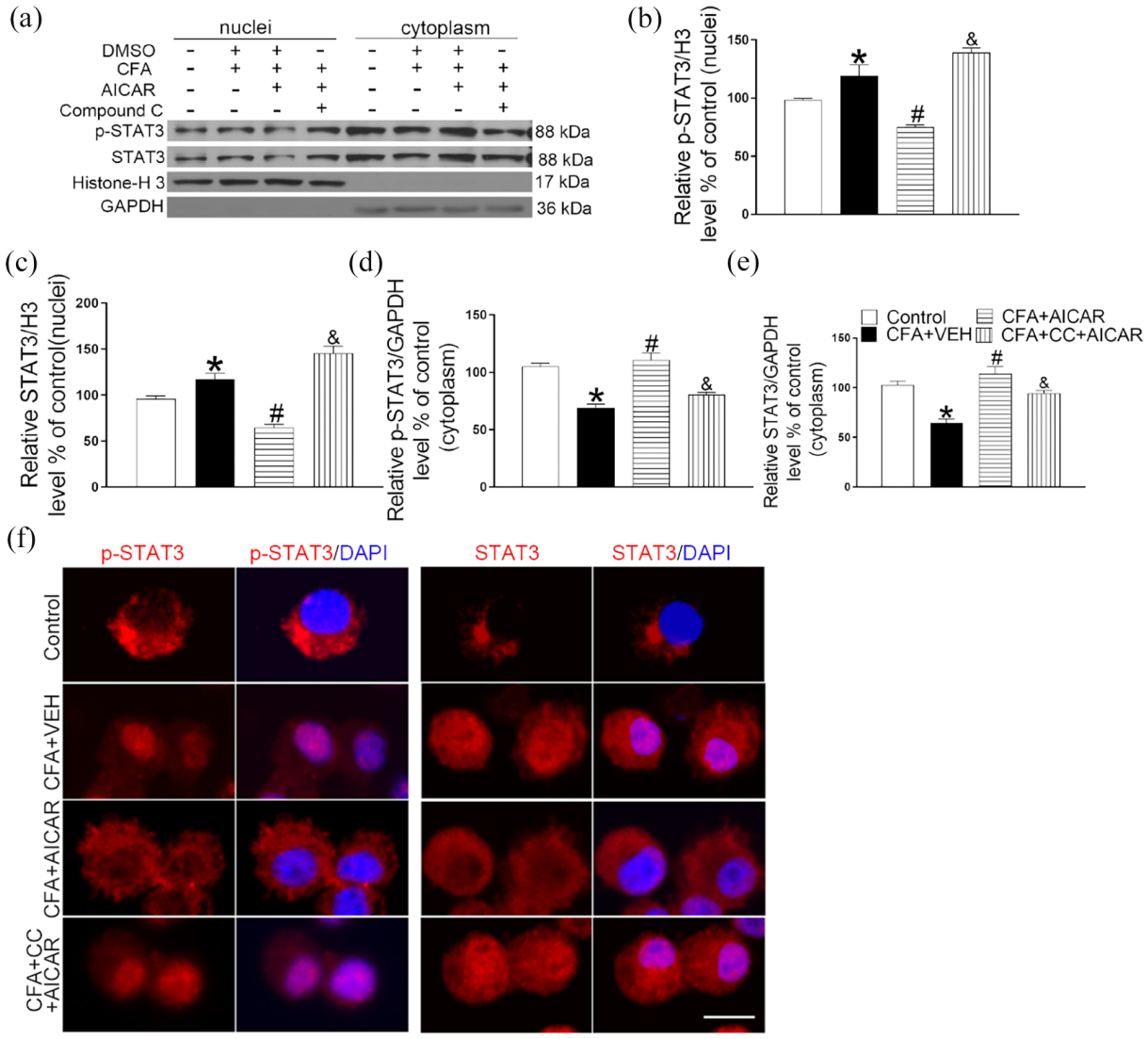

Figure 4. Activation of AMPK inhibits STAT3 nuclear translocation, reduces the level of p-STAT3 (Ser727) in the nuclei, and promotes the phosphorylation of STAT3 (Ser727) in the cytoplasm of NR8383 cells treated with CFA. Cells were collected to extract nuclear and cytoplasmic proteins for Western blot 24 h after AICAR treatment. Gel images (a) of p-STAT3(Ser727), STAT3, Histone-3 and GAPDH proteins in the cytoplasm (d and e) and nuclei (b and c) of NR8383 ($n = 3$ per group). *$p < 0.05$ versus Control group, #$p < 0.05$ versus CFA+VEH group and &$p < 0.05$ vs. CFA+AICAR group (One-way ANOVA). VEH is the vehicle of AICAR (0.01 M PBS). CC, Compound C. Co-localization of STAT3 and p-STAT3 (ser727) in macrophages. (f) Immunofluorescence images show the effect of CFA and AICAR on the subcellular distribution of p-STAT3 (Ser727) (red), STAT3 (red) and DAPI in NR8383 cells. Scale bar, 50 μm.

activity of STAT3.[36] In Raw 264.7 cells, LPS causes nuclear translocation of STAT3, and p-STAT3 (Ser727) promotes the transcription of iNOS in nuclei.[37] In LPS-induced RAW264.7 macrophages, LPS can mediate the activation of Janus kinase 2 and the phosphorylation of STAT3 at Ser727 and Tyr705 sites, promoting the expression of inflammatory factors including iNOS. Resokaempferol exerts its anti-inflammatory effects by suppressing the activation of the NF-κB and STAT3 pathways, thereby inhibiting their nuclear translocation and consequently downregulating the expression of inflammatory cytokines.[38] In LPS-induced sepsis rat model, the activation of STAT3 by miR-34a mediates the expression and secretion of iNOS in pulmonary macrophages.[39]

Our study showed that CFA induced the up-regulation of iNOS and increased phosphorylation of STAT3 (Ser727). AICAR alleviated CFA-induced pain hypersensitivity, and inhibited iNOS expression in CFA-induced inflammatory skin tissues. Contrary to our hypothesis, we found that AICAR promoted the phosphorylation of STAT3(Ser727). Interestingly, our further study found that AICAR inhibited the level of STAT3 and p-STAT3(Ser727) in the nuclei, and increased the level of p-STAT3(Ser727) in the cytoplasmic

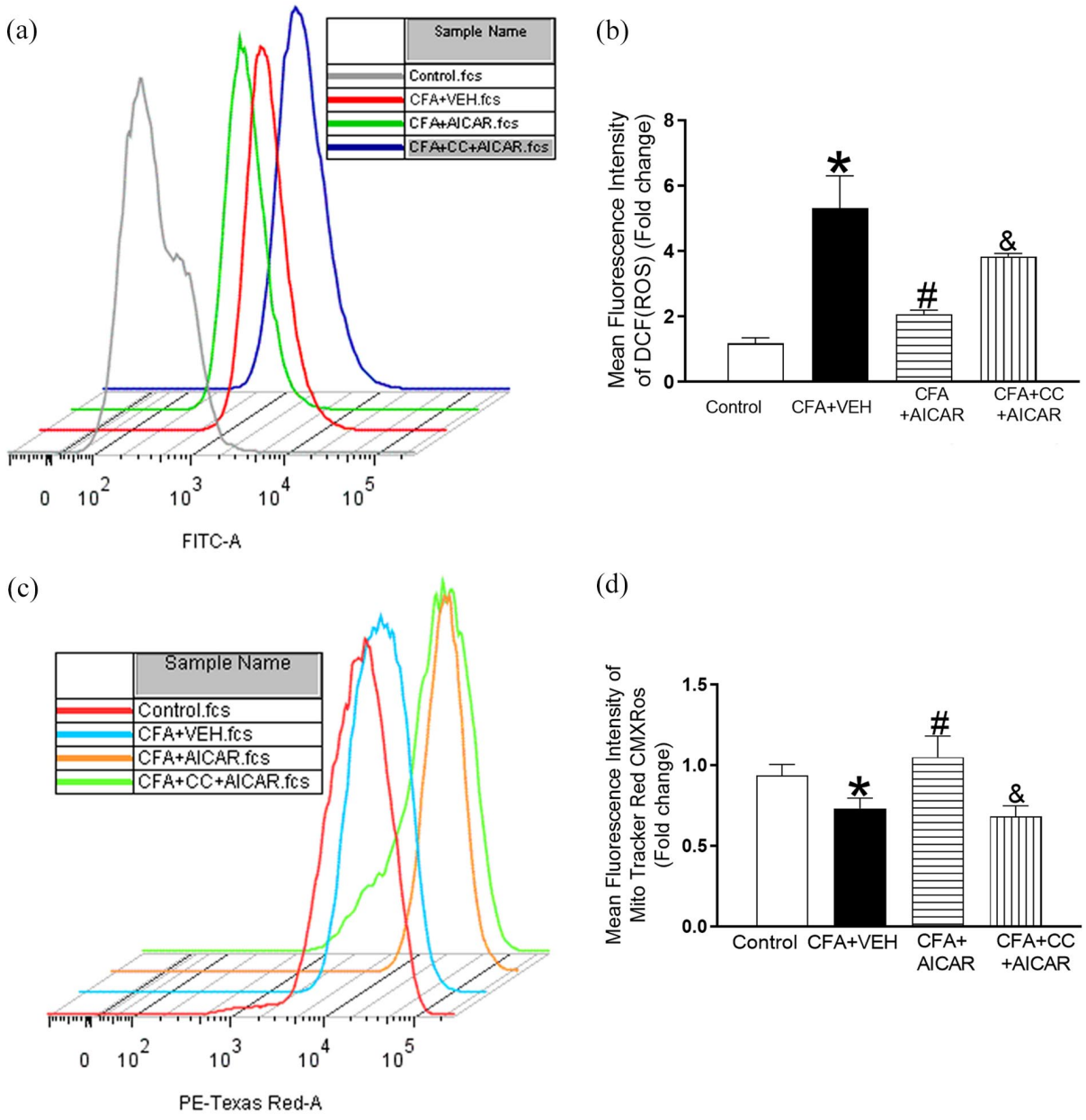

Figure 5. Activation of AMPK attenuates ROS accumulation and mitochondrial damage induced by CFA in NR8383 cells. Peak histograms (a) and group data (b) of DCFDA fluorescence intensity ($n = 3$ per group). Peak histograms **(C)** and group data (d) of fluorescence intensity Mito tracker red CMXRos ($n = 3$ per group). Cells were collected and stained with DCFDA and Mito tracker red CMXRos for flow cytometry 24 h after AICAR treatment. *$p < 0.05$ versus Control group, #$p < 0.05$ versus CFA+VEH group and & $P < 0.05$ vs. CFA+AICAR group (one-way ANOVA). VEH is the vehicle of AICAR (0.01 M PBS). CC, Compound C.

protein of inflammatory skin tissues. In vitro studies utilized NR8383 macrophages as the cell model for experimentation. CFA induced NR8383 macrophages inflammatory response and increased iNOS expression. Meanwhile, CFA increased the level of STAT3 and p-STAT3(Ser727) in the nuclei. AICAR inhibited the level of STAT3 and p-STAT3(Ser727) in the nuclei, and increased the level of p-STAT3(Ser727) in the cytoplasm in NR8383 macrophages after CFA treatment. Compound C reversed the effects of AICAR. In vitro experiments, CFA induced a decrease of total p-STAT3(Ser727) level in NR8383 cells. It contradicts the experimental outcomes observed in vivo. According to previous studies, promoting phosphorylation of STAT3 Ser727 leads to dephosphorylation of Y705 to inhibit STAT3 nuclear translocation.[40,41] To sum up, we still concluded that AMPK activation inhibited the increase of STAT3 and p-STAT3(Ser727) in the nuclei to increase the expression of iNOS. However, whether STAT3 directly or indirectly regulates the expression of iNOS (*nos2*) upon nuclear translocation requires further investigation.

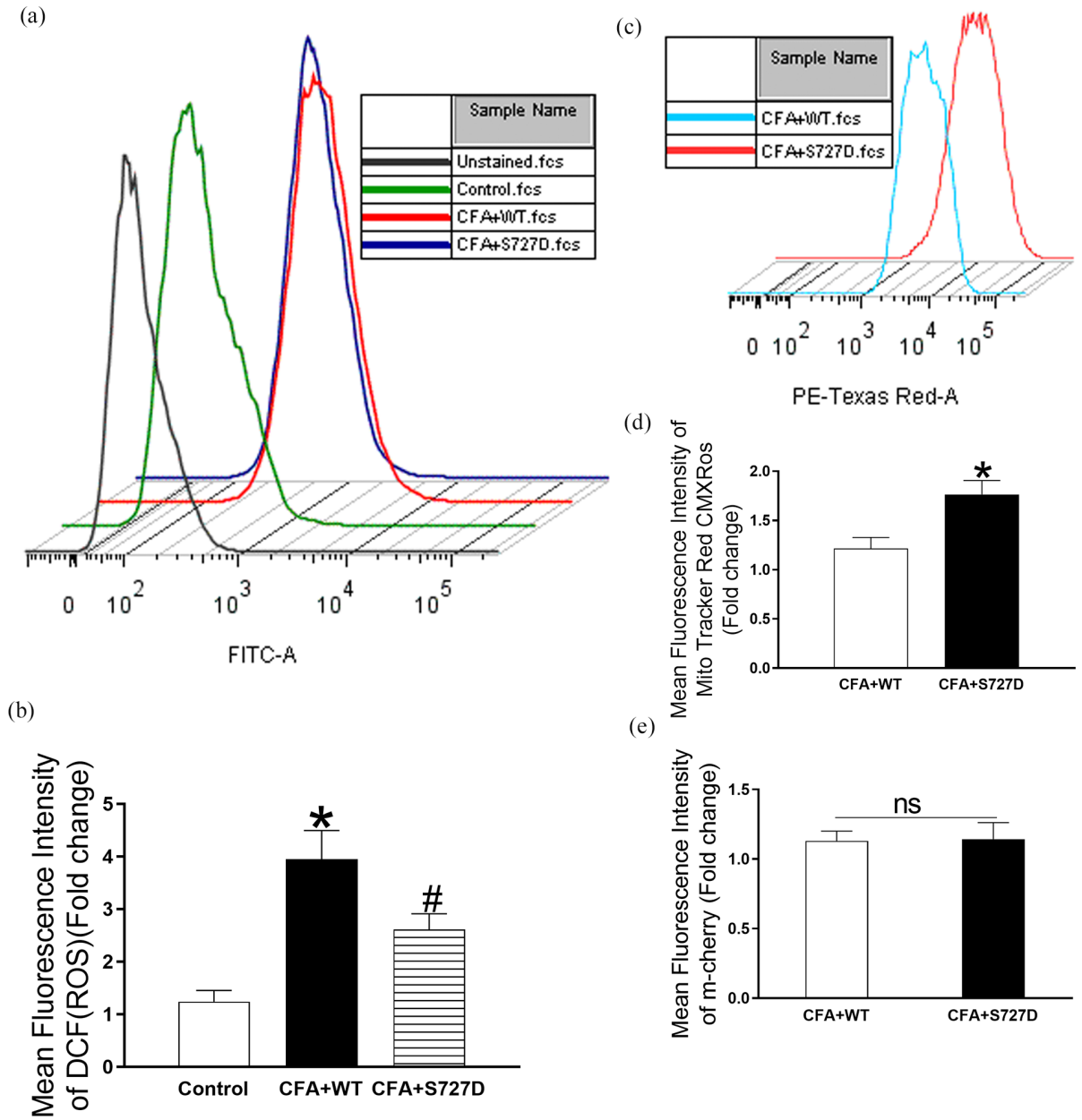

Figure 6. Promoting STAT3 phosphorylation attenuates ROS accumulation and mitochondrial damage induced by CFA in NR8383 cells. (a, b) Peak histogram and group data of DCF fluorescence intensity ($n = 3$ per group). (c, d) Peak histogram and group data of Mito Tracker Red CMXRos ($n = 3$ per group). NR8383 cells were transfected with wild-type (m-Cherry-STAT3 WT) or the STAT3 Ser727 mutant (m-Cherry-STAT3 S727D) vectors, and then the cells were treated with CFA (100 μg/ml) for 24 h before flow cytometry. *$p < 0.05$ vs. Control group and #$p < 0.05$ versus CFA+WT group (One-way ANOVA in b or unpaired Student's t test in d and e). *$p < 0.05$ versus Control group ($n = 3$ per group). (e) m-Cherry fluorescence intensity of CFA+WT group and CFA+S727D group without Mito Tracker Red CMXRos staining.

In addition, AMPK activation increased p-STAT3 (Ser727) in cytoplasm of macrophages, which may exert anti-inflammation effect by regulating ROS accumulation. ROS are intermediate products of normal oxygen metabolism, which are involved in the regulation of cell proliferation and also have harmful effects on inflammatory mediators.[42] ROS are also involved in the occurrence of pain, such as the recruitment of CX3CR1 positive monocyte macrophages at the site of peripheral nerve injury after cancer chemotherapy, which can release ROS to activate TRPA1 (transient receptor potential ankyrin 1) channel to induce nociception.[40] In vitro experiments, NR8383 macrophages were used for cell experiments. CFA increased ROS level and mitochondrial damage in NR8383 macrophages. AICAR

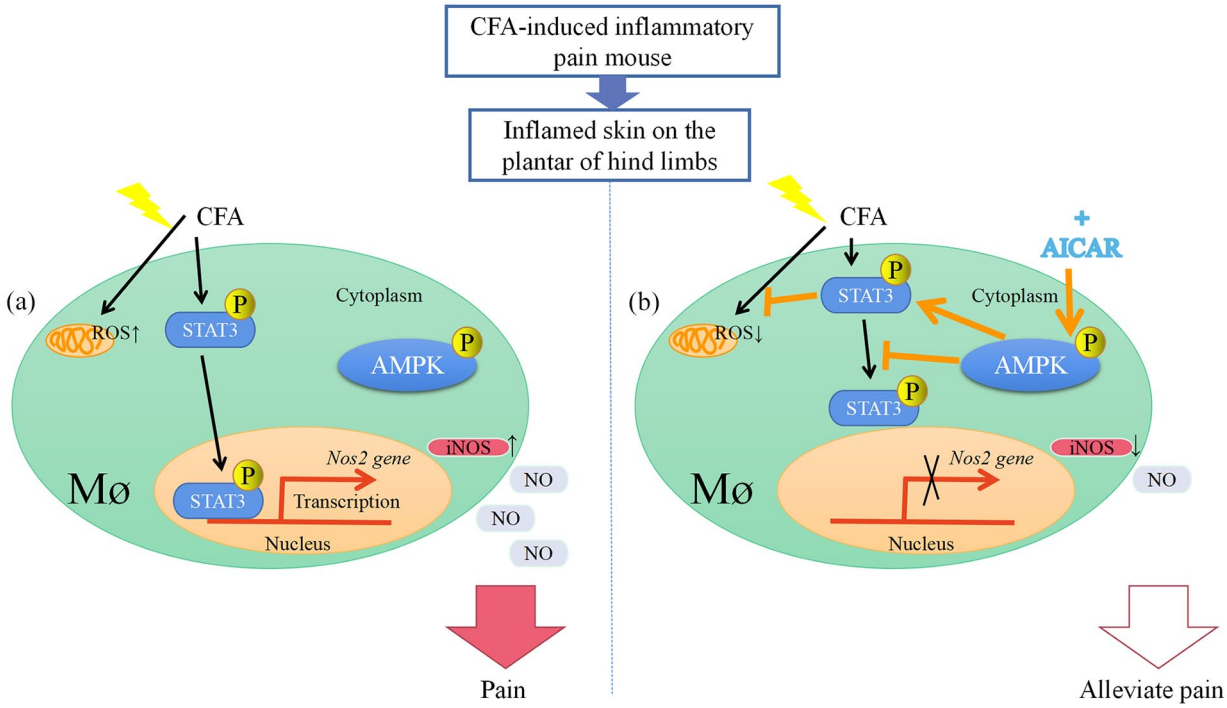

Figure 7. Schematic diagram shows that AMPK activation regulates STAT3 to alleviate inflammatory pain. (a) In CFA-induced inflammatory pain model, CFA causes STAT3 nuclear translocation in macrophages and increases the level of p-STAT3 (Ser727) in the nuclei to promote the expression of iNOS(*Nos2 gene*). Also, CFA induces ROS accumulation and mitochondrial dysfunction in macrophages. (b) Activating AMPK with AICAR inhibits STAT3 nuclear translocation and decreases p-STAT3 (Ser727) in the nuclei to reduce iNOS in macrophages. Activation of AMPK increases p-STAT3 (Ser727) in the cytoplasm to attenuate CFA-induced mitochondrial damage and ROS accumulation.

inhibited the level of ROS and alleviated mitochondrial damage after CFA treatment. Compound C reversed the effects of AICAR.

Macrophages, pivotal in modulating inflammation and pain, assume distinct roles in both the induction and resolution of pain.[43,44] Macrophage polarization is a critical determinant in the genesis and alleviation of pain. M1 macrophages, which are quasi-activator types, generate pro-inflammatory cytokines that enhance the sensitivity of pain receptors, potentially instigating inflammatory pain. Conversely, M2 macrophages, characterized as anti-inflammatory, secrete cytokines that counter inflammation, foster tissue repair, and aid in the dissipation of pain.[45,46] Macrophages, as phagocytes, clear dead and dying cells through efferocytosis, preventing secondary necrosis and exacerbation of inflammation, thereby facilitating the resolution of inflammation.[47,48] Additionally, phagocytosis leads to a reduction in the production of pro-inflammatory cytokines by macrophages and an increase in the expression of specialized pro-resolving mediators (SPMs) and anti-inflammatory cytokines, such as IL-10.[49,50] In a CFA-induced model of inflammatory pain, day 7 is a critical time point for peripheral inflammation in animals. Electroacupuncture can inhibit the activation of NOD-like receptor family pyrin domain containing 3 (NLRP3) inflammasome in macrophages in inflammatory skin tissue.[51] Maresin 1 (MaR1), a pro-resolving mediator produced by macrophages, has been found to stimulate macrophage phagocytosis, wound regeneration, and control both inflammatory and neuropathic pain.[2] In chronic pain conditions, there is no significant disparity in the total macrophage population between sexes.[52] However, in chronic pain caused by inflammation activated by the innate immune system, female mice are more sensitive to the effects of macrophages.[53,54] Sex can directly affect the activation status of macrophages. In the research on the mechanism by which allopregnanolone inhibits cytokines/chemokines, it has been observed that allopregnanolone suppresses TLR4 activation in both males and females. However, the inhibition of TLR7 signaling exhibits specificity toward female donors.[55] Our study utilized adult male mice to investigate the potential mechanism by which AMPK-STAT participates in the regulation of macrophage inflammatory cytokine iNOS expression to exert analgesic effects. Further research is warranted on the role of AMPK-STAT in macrophage polarization, efferocytosis, and the implications of gender differences in analgesic mechanisms.

ROS in CFA group significantly increased, and the fluorescence intensity of Mito tracker red CMXRos significantly decreased. Compared with CFA group, ROS fluorescence intensity of CFA plus AICAR group significantly decreased,

the fluorescence intensity of Mito tracker red CMXRos significantly increased. Compound C significantly reversed the effect of AICAR. This study showed that CFA induced ROS accumulation and mitochondrial damage in macrophages, and specific activation of AMPK significantly attenuated ROS accumulation and mitochondrial damage induced by CFA. According to the previous reports, the Ser727 site of STAT3 was mutated to aspartate(STAT3 S727D) as continuous phosphorylation of STAT3.[15,24] STAT3 S727D significantly attenuated ROS accumulation and mitochondrial damage induced by CFA. In this study, AMPK specific activation promotes the phosphorylation of STAT3 Ser727 in the cytoplasm to reduce the ROS accumulation and mitochondrial damage induced by CFA. After nerve injury, the production of NO can activate glial cells and infiltrating macrophages, which induce prolonged iNOS transcription in response to nerve damage. iNOS can lead to excessive neuronal excitability. In the spared nerve injury rat model, intraperitoneal injection of the iNOS inhibitor 1400W can improve pain behavior, while inhibiting the inflammatory factors iNOS, IL-1β, and IL-1α to exert analgesic effects.[56] In the formalin-induced pain mouse model, 2,2'-dipyridyl diselenide can significantly improve pain behavior while inhibiting the expression of spinal iNOS, NF-κB, and JNK phosphorylation.[57] iNOS-derived NO enhances the production of mitochondrial ROS, which diffuses into the cytoplasm and further upregulate iNOS.[58] In this study, the activation of AMPK can inhibit the production of iNOS and ROS in macrophages, thereby improving CFA-induced inflammatory pain. However, the interrelationship between iNOS and ROS and their mechanisms in regulating inflammatory pain still requires further investigation.

Conclusions

In summary, we have delineated the mechanism by which AMPK activation regulates STAT3 to ameliorate inflammatory pain in the CFA-induced inflammatory pain model. AMPK activation inhibited the nuclear translocation of STAT3, and reduced the phosphorylation of STAT3 (Ser727) within macrophage nuclei, subsequently decreasing the elevated expression of iNOS. Furthermore, AMPK activation enhanced the phosphorylation of STAT3(Ser727) in the macrophage cytoplasm, thereby mitigating ROS accumulation and mitochondrial damage. Our identification of a novel AMPK-mediated regulatory mechanism involving STAT3 and p-STAT3 (Ser727) in the mitigation of inflammatory pain offers new perspectives for pain treatment and research.

Author contributions statement

ML, GWC, WTL and NNY designed all the experiments. HCX performed the behavioral tests, qPCR, immunofluorescence, and western blotting, analyzed the data and drafted the manuscript; YYL assisted with the EA treatment and Lentivirus infection; TW and ZY helped to perform the cell culture experiments and analyze the data. HLP, LH and RJQ edited the manuscript. HPL, YML, XFH, WQG and HZ helped to revise the article. All the experiments were supervised by ML. All authors approved the final version of the manuscript.

Data availability statement

The original contributions presented in the study are included in the article, and further inquiries can be directed to the corresponding authors.

Declaration of Conflicting Interests

The author(s) declared no potential conflicts of interest with respect to the research, authorship, and/or publication of this article.

Funding

The author(s) disclosed receipt of the following financial support for the research, authorship, and/or publication of this article: This work was supported by the National Natural Science Foundation of China (No. 81973949, No. 82305049).

Ethical considerations

All experimental procedures were reviewed and approved by Animal Care and Use Committee at Huazhong University of Science and Technology (2022 Ethics No.3603) and conformed to the ethical guidelines of the International Association for the Study of Pain.

ORCID iDs

Hui-Lin Pan https://orcid.org/0000-0001-8444-3770
Man Li https://orcid.org/0000-0003-4041-0437

Reference

1. Wu M, Song W, Zhang M, et al. Potential mechanisms of exercise for relieving inflammatory pain: a literature review of animal studies. *Front Aging Neurosci* 2024; 16: 1359455.
2. Hwang SM, Chung G, Kim YH, et al. The role of maresins in inflammatory pain: function of macrophages in wound regeneration. *Int J Mol Sci* 2019; 20(23): 5849.
3. Liao HY, Hsieh CL, Huang CP, et al. Electroacupuncture attenuates CFA-induced inflammatory pain by suppressing Nav1.8 through S100B, TRPV1, Opioid, and adenosine pathways in mice. *Sci Rep* 2017; 7: 42531.
4. Vendramini-Costa DB, Spindola HM, de Mello GC, et al. Anti-inflammatory and antinociceptive effects of racemic goniothalamin, a styryl lactone. *Life Sci* 2015; 139: 83–90.
5. Qin BH, Liu XQ, Yuan QY, et al. Anti-inflammatory triterpenoids from the caulophyllum robustum maximin LPS-stimulated RAW264.7 cells. *Molecules* 2018; 23(5): 1149.
6. Oh SH, Lee HY, Ki YJ, et al. Gabexate mesilate ameliorates the neuropathic pain in a rat model by inhibition of proinflammatory cytokines and nitric oxide pathway via suppression of nuclear factor-kappaB. *Korean J Pain* 2020; 33(1): 30–39.
7. Penugurti V, Manne RK, Bai L, et al. AMPK: The energy sensor at the crossroads of aging and cancer. *Semin Cancer Biol* 2024; 106–107: 15–27.

8. Xie G, Liang Y, Gao W, et al. Artesunate alleviates intracerebral haemorrhage secondary injury by inducing ferroptosis in M1-polarized microglia and suppressing inflammation through AMPK/mTORC1/GPX4 pathway. *Basic Clin Pharmacol Toxicol* 2023; 132(5): 369–383.
9. Fu LY, Yang Y, Li RJ, et al. Activation AMPK in hypothalamic paraventricular nucleus improves renovascular hypertension through ERK1/2-NF-kappaB pathway. *Cardiovasc Toxicol* 2024; 24(9): 904–917.
10. Rutherford C, Speirs C, Williams JJ, et al. Phosphorylation of Janus kinase 1 (JAK1) by AMP-activated protein kinase (AMPK) links energy sensing to anti-inflammatory signaling. *Sci Signal* 2016; 9(453): ra109.
11. Kim DY, Lim SG, Suk K, et al. Mitochondrial dysfunction regulates the JAK-STAT pathway via LKB1-mediated AMPK activation ER-stress-independent manner. *Biochem Cell Biol* 2020; 98(2): 137–144.
12. Xiang HC, Lin LX, Hu XF, et al. AMPK activation attenuates inflammatory pain through inhibiting NF-kappaB activation and IL-1beta expression. *J Neuroinflammation* 2019; 16(1): 34.
13. Zhang W, Li D, Li B, et al. STAT3 as a therapeutic target in the metformin-related treatment. *Int Immunopharmacol* 2023; 116: 109770.
14. Hillmer EJ, Zhang H, Li HS, et al. STAT3 signaling in immunity. *Cytokine Growth Factor Rev* 2016; 31: 1–15.
15. Dunn JD, Alvarez LA, Zhang X, et al. Reactive oxygen species and mitochondria: a nexus of cellular homeostasis. *Redox Biol* 2015; 6: 472–485.
16. Gong Y, Qiu J, Jiang T, et al. Maltol ameliorates intervertebral disc degeneration through inhibiting PI3K/AKT/NF-kappaB pathway and regulating NLRP3 inflammasome-mediated pyroptosis. *Inflammopharmacology* 2023; 31(1): 369–384.
17. Kumatia EK, Antwi S and Asase A. Analgesic and anti-inflammatory activities of NPK 500 capsules, a Cassia sieberiana DC. - Based herbal analgesic medicine used to treat dysmenorrhea and peptic ulcer, is mediated through the inhibition of PGE2 and iNOS. *J Ethnopharmacol* 2024; 333: 118510.
18. Ilari S, Giancotti LA, Lauro F, et al. Antioxidant modulation of sirtuin 3 during acute inflammatory pain: the ROS control. *Pharmacol Res* 2020; 157: 104851.
19. Zimmermann M. Ethical guidelines for investigations of experimental pain in conscious animals. *Pain* 1983; 16(2): 109–110.
20. Chaplan SR, Bach FW, Pogrel JW, et al. Quantitative assessment of tactile allodynia in the rat paw. *J Neurosci Methods* 1994; 53(1): 55–63.
21. Chen G, Kim YH, Li H, et al. PD-L1 inhibits acute and chronic pain by suppressing nociceptive neuron activity via PD-1. *Nat Neurosci* 2017; 20(7): 917–926.
22. D'Annessa I, Gandaglia A, Brivio E, et al. Tyr120Asp mutation alters domain flexibility and dynamics of MeCP2 DNA binding domain leading to impaired DNA interaction: atomistic characterization of a Rett syndrome causing mutation. *Biochim Biophys Acta Gen Subj* 2018; 1862(5): 1180–1189.
23. Hawley SA, Russell FM, Ross FA, et al. BAY-3827 and SBI-0206965: potent AMPK inhibitors that paradoxically increase Thr172 phosphorylation. *Int J Mol Sci* 2023; 25(1): 453.
24. Baeza-Flores GD, Guzmán-Priego CG, Parra-Flores LI, et al. Metformin: a prospective alternative for the treatment of chronic pain. *Front Pharmacol* 2020; 11: 558474.
25. Nan FB, Gu YX, Wang JL, et al. Electroacupuncture promotes macrophage/microglial M2 polarization and suppresses inflammatory pain through AMPK. *Neuroreport* 2024; 35(6): 343–351.
26. Peixoto CA, de Oliveira WH, da Racho Araújo SM, et al. AMPK activation: role in the signaling pathways of neuroinflammation and neurodegeneration. *Exp Neurol* 2017; 298(Pt A): 31–41.
27. Melemedjian OK, Asiedu MN, Tillu DV, et al. Targeting adenosine monophosphate-activated protein kinase (AMPK) in preclinical models reveals a potential mechanism for the treatment of neuropathic pain. *Mol Pain* 2011; 7: 70.
28. Burton MD, Tillu DV, Mazhar K, et al. Pharmacological activation of AMPK inhibits incision-evoked mechanical hypersensitivity and the development of hyperalgesic priming in mice. *Neuroscience* 2017; 359: 119–129.
29. Russe OQ, Möser CV, Kynast KL, et al. Activation of the AMP-activated protein kinase reduces inflammatory nociception. *J Pain* 2013; 14(11): 1330–1340.
30. Zhao X, Li Y, Lin X, et al. Ozone induces autophagy in rat chondrocytes stimulated with IL-1beta through the AMPK/mTOR signaling pathway. *J Pain Res* 2018; 11: 3003–3017.
31. Saragusti AC, Bustos PS, Pierosan L, et al. Involvement of the L-arginine-nitric oxide pathway in the antinociception caused by fruits of Prosopis strombulifera (Lam.) Benth. *J Ethnopharmacol* 2012; 140(1): 117–122.
32. Orecchioni M, Ghosheh Y, Pramod AB, et al. Macrophage polarization: different gene signatures in M1(LPS+) vs. classically and M2(LPS-) vs. alternatively activated macrophages. *Front Immunol* 2019; 10: 1084.
33. Yang J, Kunimoto H, Katayama B, et al. Phospho-Ser727 triggers a multistep inactivation of STAT3 by rapid dissociation of pY705-SH2 through C-terminal tail modulation. *Int Immunol* 2020; 32(2): 73–88.
34. Akira S, Nishio Y, Inoue M, et al. Molecular cloning of APRF, a novel IFN-stimulated gene factor 3 p91-related transcription factor involved in the gp130-mediated signaling pathway. *Cell* 1994; 77(1): 63–71.
35. Levy DE, Darnell Jr JE. Stats: transcriptional control and biological impact. *Nat Rev Mol Cell Biol* 2002; 3(9): 651–662.
36. Andrés RM, Hald A, Johansen C, et al. Studies of Jak/STAT3 expression and signalling in psoriasis identifies STAT3-Ser727 phosphorylation as a modulator of transcriptional activity. *Exp Dermatol* 2013; 22(5): 323–328.
37. Park SY, Baik YH, Cho JH, et al. Inhibition of lipopolysaccharide-induced nitric oxide synthesis by nicotine through S6K1-p42/44 MAPK pathway and STAT3 (Ser 727) phosphorylation in Raw 264.7 cells. *Cytokine* 2008; 44(1): 126–134.
38. Yu Q, Zeng K, Ma X, et al. Resokaempferol-mediated anti-inflammatory effects on activated macrophages via the inhibition of JAK2/STAT3, NF-kappaB and JNK/p38 MAPK signaling pathways. *Int Immunopharmacol* 2016; 38: 104–114.
39. Cheng DL, Fang HX, Liang Y, et al. MicroRNA-34a promotes iNOS secretion from pulmonary macrophages in septic suckling rats through activating STAT3 pathway. *Biomed Pharmacother* 2018; 105: 1276–1282.
40. Malcangio M. Role of the immune system in neuropathic pain. *Scand J Pain* 2019; 20(1): 33–37.
41. Wakahara R, Kunimoto H, Tanino K, et al. Phospho-Ser727 of STAT3 regulates STAT3 activity by enhancing

dephosphorylation of phospho-Tyr705 largely through TC45. *Genes Cells* 2012; 17(2): 132–145.
42. Gupta S, Goldberg JM, Aziz N, et al. Pathogenic mechanisms in endometriosis-associated infertility. *Fertil Steril* 2008; 90(2): 247–257.
43. Bang S, Xie YK, Zhang ZJ, et al. GPR37 regulates macrophage phagocytosis and resolution of inflammatory pain. *J Clin Invest* 2018; 128(8): 3568–3582.
44. Menon N, Kishen A. Nociceptor-macrophage interactions in apical periodontitis: how biomolecules link inflammation with pain. *Biomolecules* 2023; 13(8): 1193.
45. Xu YD and Liang XC, Li ZP, et al. Apoptotic body-inspired nanotherapeutics efficiently attenuate osteoarthritis by targeting BRD4-regulated synovial macrophage polarization. *Biomaterials* 2024; 306: 122483.
46. Jie L, Zhang L, Fu H, et al. Xibining inhibition of the PI3K-AKT pathway reduces M1 macrophage polarization to ameliorate KOA synovial inflammation and nociceptive sensitization. *Phytomedicine* 2024; 136: 156281.
47. Schilperoort M, Ngai D, Sukka SR, et al. The role of efferocytosis-fueled macrophage metabolism in the resolution of inflammation. *Immunol Rev* 2023; 319(1): 65–80.
48. Bäck M, Yurdagul Jr A, Tabas I, et al. Inflammation and its resolution in atherosclerosis: mediators and therapeutic opportunities. *Nat Rev Cardiol* 2019; 16(7): 389–406.
49. Zhang Q, Bang S, Chandra S, et al. Inflammation and infection in pain and the role of GPR37. *Int J Mol Sci* 2022; 23(22): 14426.
50. Sukka SR, Ampomah PB, Darville LN, et al. Efferocytosis drives a tryptophan metabolism pathway in macrophages to promote tissue resolution. *Nat Metab* 2024; 6(9): 1736–1755.
51. Gao F, Xiang HC, Li HP, et al. Electroacupuncture inhibits NLRP3 inflammasome activation through CB2 receptors in inflammatory pain. *Brain Behav Immun* 2018; 67: 91–100.
52. Chen O, Luo X and Ji RR. Macrophages and microglia in inflammation and neuroinflammation underlying different pain states. *Med Rev* 2023; 3(5): 381–407.
53. Friedman TN, La Caprara O, Zhang C, et al. Sex differences in peripheral immune cell activation: Implications for pain and pain resolution. *Brain Behav Immun* 2023; 114: 80–93.
54. Liu L, Karagoz H, Herneisey M, et al. Sex differences revealed in a mouse CFA inflammation model with macrophage targeted nanotheranostics. *Theranostics* 2020; 10(4): 1694–1707.
55. Balan I, Aurelian L, Williams KS, et al. Inhibition of human macrophage activation via pregnane neurosteroid interactions with toll-like receptors: sex differences and structural requirements. *Front Immunol* 2022; 13: 940095.
56. Sobeh M, Mahmoud MF, Rezq S, et al. Haematoxylon campechianum extract ameliorates neuropathic pain via inhibition of NF-kappaB/TNF-alpha/NOX/iNOS signalling pathway in a rat model of chronic constriction injury. *Biomolecules* 2020; 10(3); 45.
57. Rosa SG, Brüning CA, Pesarico AP, et al. Anti-inflammatory and antinociceptive effects of 2,2;-dipyridyl diselenide through reduction of inducible nitric oxide synthase, nuclear factor-kappa B and c-Jun N-terminal kinase phosphorylation levels in the mouse spinal cord. *J Trace Elem Med Biol* 2018; 48: 38–45.
58. Anavi S and Tirosh O. iNOS as a metabolic enzyme under stress conditions. *Free Radic Biol Med* 2020; 146: 16–35.